# Definitive hematopoiesis initiates through a committed erythromyeloid progenitor in the zebrafish embryo

Julien Y. Bertrand*, Albert D. Kim*, Emily P. Violette, David L. Stachura, Jennifer L. Cisson and David Traver[†]

Shifting sites of blood cell production during development is common across widely divergent phyla. In zebrafish, like other vertebrates, hematopoietic development has been roughly divided into two waves, termed primitive and definitive. Primitive hematopoiesis is characterized by the generation of embryonic erythrocytes in the intermediate cell mass and a distinct population of macrophages that arises from cephalic mesoderm. Based on previous gene expression studies, definitive hematopoiesis has been suggested to begin with the generation of presumptive hematopoietic stem cells (HSCs) along the dorsal aorta that express *c-myb* and *runx1*. Here we show, using a combination of gene expression analyses, prospective isolation approaches, transplantation, and in vivo lineage-tracing experiments, that definitive hematopoiesis initiates through committed erythromyeloid progenitors (EMPs) in the posterior blood island (PBI) that arise independently of HSCs. EMPs isolated by coexpression of fluorescent transgenes driven by the *lmo2* and *gata1* promoters exhibit an immature, blastic morphology and express only erythroid and myeloid genes. Transplanted EMPs home to the PBI, show limited proliferative potential, and do not seed subsequent hematopoietic sites such as the thymus or pronephros. In vivo fate-mapping studies similarly demonstrate that EMPs possess only transient proliferative potential, with differentiated progeny remaining largely within caudal hematopoietic tissue. Additional fate mapping of mesodermal derivatives in mid-somitogenesis embryos suggests that EMPs are born directly in the PBI. These studies provide phenotypic and functional analyses of the first hematopoietic progenitors in the zebrafish embryo and demonstrate that definitive hematopoiesis proceeds through two distinct waves during embryonic development.

KEY WORDS: Erythromyeloid progenitor, Hematopoiesis, Hematopoietic progenitor cells, Zebrafish

## INTRODUCTION

The genesis of the blood-forming system is complex, with shifting sites of hematopoiesis occurring during development. The ontogeny of blood cells from multiple hematopoietic organs appears to be a feature common to all organisms with multiple hematopoietic lineages, including both invertebrates and vertebrates (Evans et al., 2003; Hartenstein, 2006). Whereas the specific organs that transiently host blood cell production can be divergent between species, hematopoiesis can be roughly divided into two major waves in vertebrates based on the cell types generated. Primitive hematopoiesis is characterized by a relatively rapid commitment of embryonic mesoderm to monopotent hematopoietic precursors (Keller et al., 1999). These cells give rise to embryonic erythrocytes and macrophages that are respectively required to oxygenate and remodel growing tissues of the embryo (Palis and Yoder, 2001). Definitive hematopoiesis is characterized by the emergence of multipotent hematopoietic stem and progenitor cells (Cumano and Godin, 2007).

The multiple waves of blood cell development have been best studied in the mouse, where hematopoiesis initiates with the formation of primitive erythrocytes and macrophages in the extraembryonic yolk sac (Palis et al., 1999). It is widely believed that definitive hematopoiesis subsequently begins in the midgestation embryo with the formation of HSCs in a region bounded by the aorta, gonads and mesonephros (AGM) (Dzierzak, 2005; Cumano and Godin, 2007). However, recent studies have demonstrated the

presence of definitive progenitors within the yolk sac (Yoder et al., 1997a; Yoder et al., 1997b; Palis et al., 1999; Bertrand et al., 2005a; Yokota et al., 2006; Yokomizo et al., 2007) and placenta (Gekas et al., 2005; Ottersbach and Dzierzak, 2005; Zeigler et al., 2006) that arise either before, or concomitant with, HSC formation in the AGM region. Several reports have shown that a common marker of definitive hematopoietic stem and progenitor cells in each of these tissues is the integrin, CD41 (Mitjavila-Garcia et al., 2002; Ferkowicz et al., 2003; Mikkola et al., 2003; Ottersbach and Dzierzak, 2005). Before embryonic day (E) 9.5, CD41^{+} yolk sac cells generate multiple myeloid and erythroid lineages, but lack lymphoid potential in co-culture assays (Yokota et al., 2006). Similar results were obtained at E10.5 using yolk sac cells purified by combined CD41^{+} c-Kit^{+} CD45^{−} expression (Bertrand et al., 2005b). In addition, studies utilizing a transgenic mouse expressing GFP under control of the *Gata1* promoter showed that *Gata1^{+}* cells purified from E7.5 yolk sacs could generate granulocytes, monocytes, macrophages and erythrocytes upon OP9 stromal cells (Yokomizo et al., 2007). Together, these studies suggest that the definitive hematopoietic program may first generate committed erythromyeloid progenitors in the yolk sac before HSCs arise. The lineage relationships and relative contributions of definitive precursors in the yolk sac to later hematopoietic sites, such as the fetal liver, fetal spleen and bone marrow remain to be clarified.

In the zebrafish, primitive hematopoiesis also produces macrophages and erythrocytes. The first functional hematopoietic cells born in the embryo are primitive macrophages. These cells arise from anterior, cephalic mesoderm then migrate onto the yolk syncitial layer before colonizing embryonic tissues (Herbomel et al., 1999). Primitive erythrocytes develop from bilateral stripes of ventral mesoderm, which, upon migration to the midline, form a structure termed the intermediate cell mass (ICM) (Detrich et al., 1995; Thompson et al., 1998). Endothelial cells encapsulate this

Section of Cell and Developmental Biology, Division of Biological Sciences, University of California, San Diego, La Jolla, CA 92093-0380, USA

*These authors contributed equally to this work
†Author for correspondence (e-mail: dtraver@ucsd.edu)

mass of maturing erythroid precursors to form the cardinal vein and, upon initiation of heart contractions at approximately 24 hours post-fertilization (hpf), primitive erythroblasts enter circulation. Based on the appearance of cells expressing HSC-associated genes such as *c-myb* and *runx1* along the ventral wall of the dorsal aorta, definitive hematopoiesis has been presumed to initiate in this zebrafish equivalent of the AGM region between 28 and 48 hpf (Thompson et al., 1998; Burns et al., 2002; Kalev-Zylinska et al., 2002). Lineage-tracing studies have recently shown that cells residing between the aorta and vein could subsequently colonize the thymus and pronephros, the major definitive hematopoietic organs in zebrafish (Murayama et al., 2006; Jin et al., 2007).

The vertebrate AGM is not a hematopoietic organ per se, because differentiation is not observed in this region (Godin et al., 1999). Rather, the differentiation of embryonic HSCs into multiple definitive lineages occurs only after the seeding of other tissues, such as the fetal liver in mammals. Until recently, it was thought that HSCs born in the zebrafish AGM colonized the pronephros to initiate definitive hematopoiesis (Hsia and Zon, 2005). Recent fate-mapping studies of Murayama et al. showed that presumptive HSCs targeted along the aorta first migrate to a region in the tail they termed caudal hematopoietic tissue (CHT) (Murayama et al., 2006). At earlier stages, before 36 hpf, this region has also been referred to as the posterior ICM (Detrich, 3rd et al., 1995; Thompson et al., 1998), ventral vein region (Liao et al., 1998; Willett et al., 1999) and more conventionally as the posterior blood island (PBI) (Crowhurst et al., 2002; Rombout et al., 2005; Kinna et al., 2006; Renshaw et al., 2006; Jin et al., 2007) based on localization of hematopoietic markers to the ventral portion of the tail immediately caudal to the yolk tube extension. Electron microscopy studies showed that definitive myeloid cells, such as neutrophilic granulocytes, are first detected in this region at 34 hpf (Willett et al., 1999). It is not clear whether these cells migrate here from other hematopoietic sites, or whether they arise in situ from resident stem or progenitor cells. Murayama and colleagues (Murayama et al., 2006) hypothesized that the CHT is generated by migration of HSCs from the AGM to act as a fetal liver equivalent in bridging definitive blood cell production until the pronephros becomes the final hematopoietic site.

In the present study, we describe a previously uncharacterized hematopoietic precursor that arises in the PBI to initiate definitive hematopoiesis. This precursor can be prospectively isolated by flow cytometry as early as 24 hpf based on the expression of fluorescent transgenes. Molecular characterization showed promiscuous expression of erythroid and myeloid genes. Accordingly, functional studies showed that these cells have erythroid and myeloid differentiation potential but lack lymphoid potential. We have therefore termed these cells erythromyeloid progenitors (EMPs). EMPs arise before HSCs were detected in the AGM, and fate-mapping studies suggest that they arise directly from $lmo2^+$ posterior lateral plate mesoderm (LPM) derivatives. Taken together, these results demonstrate that the EMP serves as a transient progenitor that is born independently of HSCs to initiate definitive hematopoiesis in the developing zebrafish embryo.

## MATERIALS AND METHODS
### Zebrafish stocks and embryos
Zebrafish were mated, staged and raised as described (Westerfield, 1994) and maintained in accordance with UCSD IACUC guidelines. Transgenic lines *Tg(gata1:DsRed)* (Traver et al., 2003), *Tg(CD41:eGFP)* (Lin et al., 2005), *Tg(lmo2:DsRed)* (Zhu et al., 2005) and *Tg(lmo2:eGFP)* (Zhu et al., 2005) were used. *Tg(mpx:eGFP)* animals were generously provided by

S. A. Renshaw (Renshaw et al., 2006). Hereafter, transgenic lines will be referred to without the *Tg(xxx:xxx)* nomenclature for clarity. Embryos were processed as described (Westerfield, 1994).

### Whole-mount RNA in situ hybridization
Embryos were treated with PTU, then fixed in 4% or 10% paraformaldehyde (PFA). Whole-mount in situ hybridization was carried out as described (Thisse et al., 1993). The zebrafish *CD45* homologue was identified on chromosome 22 (Ensembl #ENSDARG00000030937), and a 1.2 kb probe generated from genomic DNA by PCR using the following primers: *CD45*-FP: AATGAAAAGGCTGTAATCGG; *CD45*-RP: GTCCTTGTTTTCTT-CGCTGC.

### Fluorescence in situ hybridization (FISH)
Antisense mRNA probes were prepared as previously reported for *gata1*, *pu.1* (also known as *spi1* – ZFIN) and *mpx* (Rhodes et al., 2005) using digoxigenin (DIG)- or fluorescein (FITC)-labeled UTPs according to the manufacturer's instructions (Roche, Palo Alto, CA). Two-color FISH was carried out as previously described (Kosman et al., 2004) with minor modifications. The 90% xylene/10% ethanol wash was omitted and proteinase K treatments were adjusted to 25 minutes for optimal permeabilization. Hybridization with 500 ng DIG-labeled and FITC-labeled probes was performed at 70°C. *mpx*-FITC probes were detected with a mouse anti-FITC antibody (Roche) followed by a donkey anti-mouse Alexa Fluor 555 antibody (Molecular Probes). Reactions were developed using anti-DIG-horseradish peroxidase (HRP) antibody. *gata1*-FITC was detected with a mouse anti-FITC antibody (Roche) followed by a goat anti-mouse-HRP antibody (Molecular Probes, Carlsbad, CA). Alexa Fluor 488 or 594 tyramide substrates were used according to the manufacturer's instructions (Molecular Probes) to further amplify *gata1*-DIG and *pu.1*-DIG or *gata1*-FITC signals, respectively. Fluorescence images were acquired on an Olympus Fluoview 1000 confocal microscope at 200× and 400× magnification (Center Valley, PA).

### Cell suspension preparation
PTU-treated whole or dissected embryos were dissociated between 24 and 72 hpf. Embryos were treated with 10 mM DTT in E3 medium then transferred to Hank's balanced salt solution (with calcium) and digested with Liberase Blendzyme II (Sigma Aldrich, St Louis, MO) for at least 1 hour at 33°C. Cell suspensions were then filtered through 40 μm nylon mesh, washed twice and pelleted by centrifugation at 250 *g* for 5 minutes.

### Flow cytometry
Embryonic cell suspensions were prepared as described above and fluorescence-activated cell sorting (FACS) was performed as previously described (Traver et al., 2003) using a FACS Aria flow cytometer (Becton Dickinson, San Jose, CA). Data analyses were performed using FlowJo software (TreeStar, Ashland, OR).

### Cytology
Blood cells were collected by tail dissection of embryos, then homogenized using the embryonic cell collection protocol described above. Hematopoietic cells were concentrated by cytocentrifugation at 250 *g* for 5 minutes onto glass slides using a Shandon Cytospin 4 (Thermo Fischer Scientific, Waltham, MA). Slides were then processed through May-Grünwald and Giemsa stains according to the manufacturer's instructions (Fluka, Buchs, Switzerland).

### Microscopy
Embryos were imaged using a Leica DMI6000 inverted fluorescent microscope (Wetzlar, Germany), a Hamamatsu C7780 digital camera (Hamamatsu, Japan) and Volocity Acquisition and Restoration software (Improvision, Lexington, MA).

### RT-PCR analyses
For RT-PCR analysis, RNA was isolated from cells sorted from *lmo2:eGFP* and *gata1:DsRed* dual-positive embryos using Trizol (Invitrogen, Philadelphia, PA). Total RNA (2-5 μg) was reverse transcribed into cDNA using a Superscript III RT-PCR kit (Invitrogen, Philadelphia, PA). The following primers were used: *c-mpl*-FP: ATGGATCCAGTTTTCATC-TGGTGG, *c-mpl*-RP: TATAGGTAGACGTCACTTGGTGGG; *l-plastin-*

FP: GTCGATGTGGATGGGAACGG, *l-plastin*-RP: CCTCCTCGGAGT-ATGAGTGC; *CD41*-FP: TTACTACGACCTATATCTGGG, *CD41*-RP: GATGACCTGGACATACTGGG; *c-myb*-FP: AGTTACTTCCGGGAAGA-ACCG, *c-myb*-RP: AGAGCAAGTGGAAATGGCACC; *runx1*-FP: TTGG-GACGCCAAATACGAACC, *runx1*-RP: ATATCACCAAGGGCAACC-ACC; *ef1a*-FP: CGGTGACAACATGCTGGAGG, *ef1a*-RP: ACCAGTC-TCCACACGACCCA. Primers for *mpx*, *pu.1* and *gata1* transcripts were used as described (Hsu et al., 2004).

### Hematopoietic cell transplantation
Single-cell suspensions from *lmo2:eGFP*; *gata1:DsRed* transgenic embryos were prepared as described above. EMPs were sorted as described above and transplantated into 36 or 48 hpf wild-type embryos as previously described (Traver et al., 2003).

### Fate mapping
One- to eight-cell-stage *CD41:eGFP* or *lmo2:eGFP* transgenic embryos were injected with 0.5 nl of a 0:1 or 1:1 mix of caged fluorescein-dextran 10,000 MW and caged rhodamine-dextran 10,000 MW (Molecular Probes, Carlsbad, CA). Uncaging was performed using a 365 nm Micropoint laser system (Photonic Instruments, St Charles, IL) routed through the epifluorescence port and 20× objective of a Leica DMI6000 inverted microscope. Ten GFP+ target cells were uncaged per embryo following laser pulses of 10-20 seconds each. Uncaged embryos injected with rhodamine-dextran were subsequently observed using fluorescence microscopy whereas uncaged FITC was detected by immunohistochemistry, as previously described (Murayama et al., 2006).

### Generation of zebrafish kidney stromal (ZKS) cell lines
Kidneys were isolated from wild-type AB* fish by dissection and bleached for 5 minutes in 0.000525% Sodium Hypochlorite (Fisher Scientific, Pittsburgh, PA). Tissue was then rinsed in sterile Dulbecco's phosphate-buffered saline (PBS; Mediatech, Herndon, VA) and mechanically dissociated by trituration. Dissociated cells were passed through a 0.45 μM filter (BD Biosciences, San Jose, CA) and discarded. The remaining stromal cells were cultured in 12.5 cm$^2$ flasks at 32°C, 5% CO$_2$. Cells were maintained until reaching 50-80% confluency, then trypsinized (0.25%; Invitrogen, Grand Island, NY) for 10 minutes at 32°C, and split at 1:3 for expansion.

ZKS cells defined in this report were maintained in a mixture of 50% L-15, 35% DMEM, 15% Ham's F-12 media (Mediatech) supplemented with 10% FBS (American Type Culture Collection, Manassas, VA), 2% penicillin/streptomycin (10 U/ml stock), 0.1 mg/ml gentamicin sulfate, 1% L-glutamine, 150 mg/l sodium bicarbonate and 1.5% HEPES (All supplements from Mediatech).
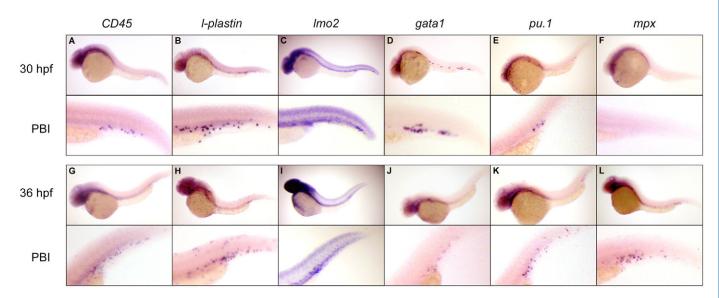
### In vitro differentiation assay
EMPs were purified by flow cytometry and plated onto confluent ZKS cells at a density of $1 \times 10^4$ cells/well in 12-well plates using 2 ml medium per well. For morphological analyses, wells were gently aspirated and 200 μl removed for cytocentrifugation onto glass slides. Cells were stained with May-Grünwald/Giemsa stains as described above, or for myeloperoxidase activity according to the manufacturer's instructions (Sigma Aldrich). Light microscopy images were obtained using an Olympus BX51 light microscope, Olympus DP70 camera, and Olympus DP Controller software (Center Valley, PA).

## RESULTS
### The posterior blood island is a site of hematopoiesis
We wished to determine when and where the first definitive hematopoietic precursors arise in the zebrafish embryo. Early gene expression studies suggested that the most posterior portion of the ICM contained hematopoietic precursors distinct from the primitive erythroblasts that arise in the ICM (Thompson et al., 1998). To determine what types of blood cells are found in the PBI, we performed whole-mount in situ hybridization (WISH) with a panel of hematopoietic genes at 30 and 36 hpf. We first identified the zebrafish homologue of *CD45*, which in mammals is expressed in all hematopoietic cell lineages except for erythrocytes. Expression of the zebrafish *CD45* gene was observed as early as 30 hpf, and positive cells increased in number by 36 hpf in the ventral part of the tail (Fig. 1A,G). Although some studies have treated *l-plastin* (also known as *lcp1* – ZFIN) as a macrophage-specific marker in the



**Fig. 1. Genes associated with multilineage hematopoiesis are expressed in the posterior blood island as early as 30 hpf.** (**A**,**B**) By 30 hpf, expression of the pan-leukocyte markers *CD45* and *l-plastin* are observed throughout the PBI. (**G**,**H**) By 36 hpf, the number of cells expressing each gene has increased in the PBI, and expressing cells begin to migrate throughout the embryo. Localized expression of *lmo2* is observed in the PBI at 30 hpf (**C**) and 36 hpf (**I**). (**D**,**J**) Expression of *gata1* is also observed in cells within the vascular plexus of the PBI at both timepoints. (**E**,**F**,**K**,**L**) Expression of genes associated with myelopoiesis is also observed within the PBI, including *pu.1* and *mpx*. Rare *pu.1*+ cells are observed at 30 hpf in the PBI (**E**) that increase in number by 36 hpf (**K**), whereas *mpx* expression is not observed until 36 hpf (**F**,**L**), consistent with it being a marker of relatively mature myelomonocytic cell types. Magnification: 100× in whole-embryo images; 300× in PBI images.

zebrafish, it is expressed in all murine leukocytes, including hematopoietic progenitors (Arpin et al., 1994; Bertrand et al., 2005b) and in zebrafish granulocytes (Meijer et al., 2007). Expression of *l-plastin* was observed in a pattern similar to that of *CD45* (Fig. 1B,H), suggesting that both genes similarly mark zebrafish leukocytes.

To assess further the possible presence of hematopoietic progenitors, we analyzed expression of *lmo2*, *gata1* and *pu.1*. *lmo2* is expressed by both vascular and hematopoietic precursors. In addition to widespread vascular staining in the tail, a small population of *lmo2*⁺ cells was observed in the PBI (Fig. 1C,I). Similarly, expression of a canonical marker of erythroid potential, *gata1*, was observed in small numbers of cells in the PBI at both time points (Fig. 1D,J). These cells did not appear to be within vessels, but rather within the vascular plexus of the PBI. *pu.1* is a transcription factor that acts as a master regulator of myeloid commitment (Tenen et al., 1997). We first observed a small population of *pu.1*⁺ cells in the PBI at 30 hpf that increased in number by 36 hpf (Fig. 1E,K). Myeloperoxidase (*mpx*) is expressed specifically in cells of the myelomonocytic lineages, and is transcriptionally controlled by Pu.1 (Tenen et al., 1997). Accordingly, *pu.1* expression precedes transcription of *mpx* in the PBI by at least 6 hours, because *pu.1* and *mpx* expression are first detected at 30 and 36 hpf, respectively (Fig. 1E,F,K,L). Expression of all genes appeared to localize to the region between the aorta and the caudal vein, just posterior to the yolk tube extension. Taken together, these data indicate that both erythroid and myeloid cells are present in the PBI at 30 hpf and are consistent with the hypothesis that the PBI is an early site of multilineage hematopoiesis.

We next took a cytological approach to determine whether definitive hematopoietic cell types could be recognized morphologically from PBI preparations. Tails were dissected from embryos at time points ranging from 24 to 72 hpf and single-cell suspensions prepared following enzymatic digestion. At 24 hpf, the only hematopoietic lineages observed were erythroblasts and rare monocytes or macrophages (see Fig. S1 in the supplementary material), each probably originating from primitive hematopoiesis. At 30 hpf another cell subset appeared that showed characteristics of early hematopoietic precursors, including blastic morphology, open chromatin structure and basophilic cytoplasm. Eosinophilic and neutrophilic granulocytes were first observed by 36 and 48 hpf, respectively. Cells of the thrombocytic series were first observed at 48 hpf, with mature thrombocytes appearing only after 72 hpf. Finally, cells displaying a lymphoblastic morphology (relatively small, round cells with scant cytoplasm) appeared at 48 hpf. Since circulating lymphocytes are not present at this time, these cells may be HSCs that have immigrated from the AGM region, consistent with the migration hypothesis of Murayama and colleagues (Murayama et al., 2006).

We performed similar analyses of hematopoietic cells present in dissected embryonic trunk and head segments. Before 48 hpf, we did not observe definitive cell types in regions other than the tail (not shown). Collectively, these hematological results demonstrate that multiple lineages of hematopoietic cells are present in the PBI, corroborating our WISH data.

## Coexpression of *lmo2* and *gata1* defines a novel hematopoietic population in the PBI

One possible explanation for the presence of definitive myeloid and erythroid cells uniquely in the PBI at 30 hpf is that they arise from local progenitor cells. In murine bone marrow, only hematopoietic stem or progenitor cells express a combination of both *Lmo2* and *Gata1* (Miyamoto et al., 2002). Since both *lmo2* and *gata1* are expressed in the PBI, we analyzed their coexpression in animals carrying *lmo2:eGFP* and *gata1:DsRed* transgenes. As shown in Fig. 2A, cells expressing high levels of both transgenes were observed in the PBI from 30-48 hpf. Flow cytometric analysis of double transgenic embryos showed a distinct population of *lmo2*⁺*gata1*⁺ cells (Fig. 2B). This population peaks in number per embryo between 30-36 hpf, the time at which the first myeloid precursors were observed by morphology (see Fig. S1 in the supplementary material). After 72 hpf, *lmo2*⁺*gata1*⁺ cells could no longer be detected (not shown).

Before 30 hpf, a population of *lmo2*^*low*^*gata1*⁺ cells was observed by flow cytometry that expressed approximately 15 times lower levels of GFP than *lmo2*⁺*gata1*⁺ cells (Fig. 2B). Cell sorting showed that the *lmo2*^*low*^*gata1*⁺ fraction consisted entirely of primitive erythroblasts (Fig. 2C, left panel). Unlike purified primitive erythoblasts, purified *lmo2*⁺*gata1*⁺ cells showed morphologies characteristic of earlier hematopoietic progenitors (Fig. 2C, middle and right panels). At 30 hpf, two morphological subtypes were present in purified *lmo2*⁺*gata1*⁺ cells. Approximately half of this population displayed a morphology characteristic of immature myelomonocytic progenitors, including asymmetric oval or bean-shaped nuclei with lightly stained cytoplasm containing darker granules (Fig. 2C, middle panel). The remaining half displayed a morphology characteristic of immature erythroid progenitors, including centered, round nuclei with stippled staining patterns and basophilic cytoplasm (Fig. 2C, right panel).

## *lmo2*⁺*gata1*⁺ cells express both erythroid and myeloid genes

Hematopoietic progenitor cells frequently express lineage markers for multiple mature cell types, reflecting their multilineage differentiation potential (Hu et al., 1997; Miyamoto et al., 2002). We therefore profiled the gene expression pattern of purified *lmo2*⁺*gata1*⁺ cells. At 30 hpf, we isolated four populations of cells defined by differential expression of *lmo2:eGFP* and *gata1:dsRed* transgenes in double transgenic embryos, including *lmo2*^*low*^*gata1*⁺, *lmo2*⁺*gata1*⁺, *lmo2*⁺*gata1*⁻ and *lmo2*⁻*gata1*⁻ fractions. In addition to expressing high levels of the erythroid-associated *gata1* reporter gene, RT-PCR analyses showed that purified *lmo2*⁺*gata1*⁺ cells expressed the pan-leukocyte marker, *l-plastin*, and the myelomonocytic genes, *mpx* and *pu.1* ('LG', Fig. 3A). By contrast, expression of these genes in purified primitive erythoblasts (*lmo2*^*low*^*gata1*⁺ cells) was undetectable ('G', Fig. 3A). This expression pattern suggests that, despite expression of the *gata1:dsRed* transgene, the *lmo2*⁺*gata1*⁺ population is not committed to the erythroid lineage. Accordingly, these cells also express *scl* and *runx1*, genes associated with early hematopoietic progenitors. Expression of the *mpx* and *runx1* genes was found in the *lmo2*⁺*gata1*⁻ fraction ('L', Fig. 3A). *runx1* is known to be expressed in endothelial cells (Kalev-Zylinska et al., 2002), the most abundant cell type marked by the *lmo2:eGFP* transgene. The presence of *mpx* transcripts may be due to low-level expression of the *lmo2:eGFP* transgene in primitive macrophages (not shown).

We also analyzed *CD41* (also known as *itga2b* – ZFIN) in each isolated subset, since its expression appears to be one of the first markers of mesoderm commitment to definitive hematopoiesis in mammals (Mitjavila-Garcia et al., 2002; Ferkowicz et al., 2003; Mikkola et al., 2003). In 30 hpf embryos, *CD41* expression was only
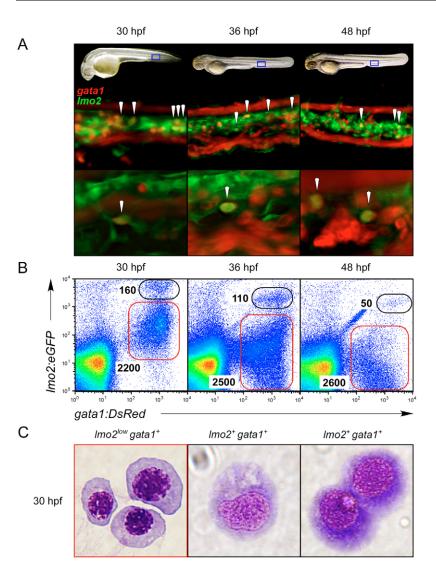
**Fig. 2. Coexpression of *lmo2* and *gata1* reveals immature hematopoietic precursors in the PBI.**
(**A**) Fluorescence microscopy reveals cells within the vascular plexus of the PBI that expressed both *gata1:DsRed* and *lmo2:eGFP* fluorophores (arrowheads) in double transgenic animals. Blue boxes in embryonic images in upper panels denote the regions shown at 200× magnification in middle and 400× magnification in lower panels at 30, 36 and 48 hpf. Lower panels show a single, deconvolved *z* slice, demonstrating coexpression of each transgene in single cells (arrowheads). (**B**) Cells coexpressing the *gata1:DsRed* and *lmo2:eGFP* transgenes prospectively isolated by flow cytometry. Double-positive cells peak in number at 30 hpf, with approximately 160 cells per embryo (left panel). (**C**) Compared with purified primitive erythroblasts sorted by low levels of *lmo2:eGFP* and high levels of *gata1:DsRed* (red gate in 30 hpf plot in B), cytological staining of purified 30 hpf *lmo2*$^+$ *gata1*$^+$ cells (black gate) showed immature morphologies indicative of early hematopoietic progenitors. Magnification, ×1000.
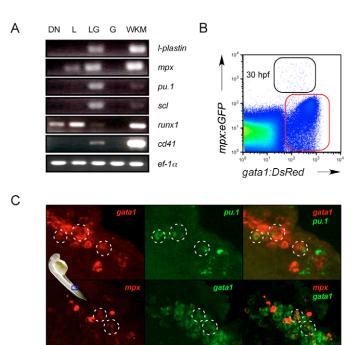
detected within *lmo2*$^+$*gata1*$^+$ cells. This result supports the hypothesis that *lmo2*$^+$*gata1*$^+$ cells represent an early definitive hematopoietic progenitor population.

To determine whether individual *lmo2*$^+$*gata1*$^+$ cells express multiple lineage markers, as would be expected for a hematopoietic progenitor cell, we performed single-cell expression studies by FACS and FISH. To assess myeloerythroid gene expression at the single-cell level, we analyzed embryos carrying *mpx:eGFP* and *gata1:DsRed* transgenes. *mpx:eGFP* transgenic zebrafish were generated recently and shown to express GFP in embryonic granulocytes (Renshaw et al., 2006). In double transgenic embryos, early expression of the *mpx:eGFP* transgene is largely localized to cells also expressing the *gata1:DsRed* transgene (Fig. 3B). We have also observed coexpression of the *mpx* and *gata1* transcripts in single cells in the PBI using two-color FISH (Fig. 3C). In murine multipotent progenitors, myeloid versus erythroid fate decisions are largely dependent upon the Pu.1 and Gata1 transcription factors, respectively (Nerlov et al., 2000; Zhang et al., 2000; Huang et al., 2007). We observed coexpression of *pu.1* and *gata1* in single cells in the PBI (Fig. 3C). We did not observe coexpression of either *pu.1* and *gata1* or *mpx* and *gata1* in any other anatomical site in the zebrafish embryo (not shown). Taken together, our gene expression analyses strongly support the existence of a definitive, multilineage precursor in the zebrafish PBI.

## PBI hematopoietic progenitors lack key characteristics of HSCs

Because *lmo2*$^+$*gata1*$^+$ cells displayed many of the features of hematopoietic progenitor cells, we wanted to test their homing, proliferative, and differentiation potentials in functional assays. *lmo2*$^+$*gata1*$^+$ cells were purified by flow cytometry from 36 hpf embryos and transplanted into WT embryonic recipients, either stage-matched or at 48 hpf. Transplanted cells homed to the PBI within 24 hours post-transplantation (Fig. 4A). In contrast to transplanted adult whole kidney marrow (WKM) cells which populate the embryonic thymus and pronephros (Traver et al., 2003), embryonic *lmo2*$^+$*gata1*$^+$ cells were never observed to seed these hematopoietic organs. Rather, donor-derived cells remained largely within the PBI and, based upon the disappearance of double-fluorescent yellow cells after 1-2 days, appeared to differentiate rapidly (Fig. 4A). Donor-derived cells were observable for approximately one week following transplantation by fluorescent transgene expression.

Several reports have demonstrated that rare, definitive hematopoietic precursors arise in the mammalian yolk sac before circulation (Palis et al., 1999; Ferkowicz et al., 2003; Bertrand et al., 2005a; Yokota et al., 2006; Yokomizo et al., 2007). These precursors express CD41 (Ferkowicz et al., 2003; Mikkola et al., 2003; Yokota et al., 2006), which appears to be the first marker of definitive

DEVELOPMENT

**Fig. 3. Gene expression profiling of hematopoietic precursors in the PBI suggest multipotency.** (**A**) Cells were purified from 30 hpf embryos by flow cytometry based on expression of *gata1:DsRed* and *lmo2:eGFP* transgenes (DN, double negative; L, *lmo2:eGFP+*, *gata1:DsRed−*; LG, *lmo2:eGFP+*, *gata1:DsRed+*; G, *lmo2:eGFP^low*, *gata1:DsRed+*; WKM, whole kidney marrow) and subjected to RT-PCR. (**B**) FACS analysis shows a population that coexpresses the *gata1:DsRed* and *mpx:eGFP* transgenes at 30 hpf (black gate). (**C**) Two-color FISH demonstrates that cells within the PBI at 30 hpf coexpress *gata1* and *pu.1* (highlighted circles, upper panels) and *gata1* and *mpx* (highlighted circles, lower panels). Blue frame on embryo denotes regions shown in C at 400× magnification.

hematopoietic commitment from mesoderm. Since *CD41* was detected only within *lmo2+gata1+* cells in 30-36 hpf embryos, we analyzed expression of *CD41:eGFP* in the PBI of transgenic embryos (Lin et al., 2005). GFP expression was detected as early as 26 hpf, and increased in intensity and in the number of cells labeled over time (not shown). The location, appearance and proliferative kinetics of *CD41+* cells closely matched those of *lmo2+gata1+* cells, suggesting that *CD41* expression represents another, independent method of detecting definitive hematopoietic precursors in the PBI.

Use of a single, GFP marker enabled lineage-tracing studies. We performed lineage-tracing experiments in living embryos by laser-targeting *CD41:eGFP+* cells to activate caged rhodamine molecules. By 40 hpf, many GFP+ cells were found within the vascular plexus of the PBI (Fig. 4B). Rhodamine was uncaged in ten *CD41:eGFP+* cells in the PBIs of 30 transgenic animals. All 30 animals displayed robust proliferation of targeted cells and distribution of their progeny throughout the PBI when analyzed at 4 days post-uncaging (Fig. 4B). However, none of the animals showed labeled progeny in the thymus (Fig. 4B, Table 1), suggesting that *CD41:eGFP+* cells in the PBI are not HSCs.

As a positive control for thymic immigration, we performed similar experiments targeting putative HSCs in the AGM region. We previously reported that *CD41:eGFP+* cells are observed between the dorsal aorta and cardinal vein in the zebrafish equivalent of the AGM (Lin et al., 2005). Based on the similarities to other vertebrate AGMs, the regional fate-mapping results of Murayama et al. (Murayama et al., 2006), and the finding that CD41 marks embryonic HSCs in the mouse (Bertrand et al., 2005b), we hypothesized that *CD41:eGFP* expression in the AGM may mark the first HSCs to arise in the zebrafish embryo. We therefore performed similar lineage-tracing studies by laser-targeting ten *CD41+* cells in the AGM. Unlike *CD41+* cells in the 40 hpf PBI, which never populated the thymus, 10/16 embryos where *CD41+* cells were targeted in the AGM between 44-48 hpf showed thymic colonization (Fig. 4B). The progeny of AGM cells were also observed to colonize the PBI, but we never observed the progeny of PBI-targeted *CD41+* cells to colonize the AGM, thymus or pronephros.

Our transplantation and fate-mapping experiments demonstrated that hematopoietic progenitors in the PBI lack lymphoid potential – a hallmark of HSCs. However, PBI progenitors did display transient but relatively robust proliferation potential. To assess the differentiation potential of these cells, we developed in vitro culture assays using a new zebrafish kidney stromal (ZKS) cell line. *lmo2+gata1+* cells were purified from 30 hpf embryos and deposited onto ZKS layers. Aliquots were removed daily and analyzed for cellular morphology. Compared to the immature morphology of uncultured cells (Fig. 2C), *lmo2+gata1+* cells rapidly differentiated into erythroid and myelomonocytic cell fates upon 2 days of culture (Fig. 4C). An approximately equivalent ratio of erythroid to myelomonocytic cells was observed on day 2 (see Fig. S2 in the supplementary material). By day 4 of culture myelomonocytic cells predominated, with most erythroid cells presumably having differentiated and died (see Fig. S2 in the supplementary material). Based on morphological analyses, cultured *lmo2+gata1+* cells

**Table 1. Fate mapping of hematopoietic precursors by laser uncaging**

*Laser activation of caged rhodamine/FITC in transgenic cd41:eGFP+ cells*

| Tissue | Stage (hpf) | n | Marked progeny in PBI | Marked progeny in thymus |
|---|---|---|---|---|
| PBI | 40 | 30 | 30 | 0 |
| | 44 | 40 | 40 | 5 |
| | 48 | 7 | 7 | 1 |
| AGM | 44 | 8 | 6 | 5 |
| | 48 | 8 | 8 | 5 |

*Laser activation of caged rhodamine/FITC in transgenic lmo2:eGFP+ cells*

| Tissue | Fixation (hpf) | n | Marked progeny in PBI | Marked progeny in trunk |
|---|---|---|---|---|
| Posterior | 30 | 8 | 5 | 0 |
| Medial | 30 | 8 | 0 | 8 |

In each experiment, 10 GFP+ cells were laser targeted to uncage a combination of rhodamine and FITC. Marked progeny were followed in living animals by rhodamine fluorescence and were detected at noted timepoints following fixation and antibody visualization. Cells targeted in *lmo2:eGFP* animals were either in medial GFP+ stripes (bounded by somites 1-10) or at the posterior-most end of the GFP expression domain.
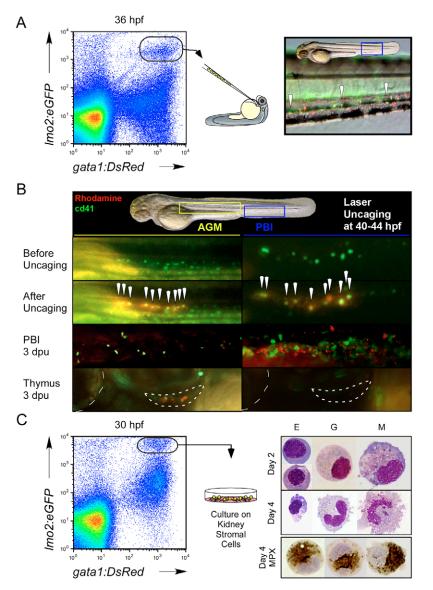
generated multiple myeloid lineages, including neutrophilic granulocytes, monocytes and macrophages (Fig. 4C), whereas parallel experiments using purified $lmo2^{low}gata1^+$ primitive erythroblasts showed only erythroid progeny (not shown). Cells were also removed after 4 days of culture and stained for myeloperoxidase (MPX) activity. Many cells demonstrated robust staining, and nuclear morphology showed that positive cells included both immature myelomonocytic cells and mature granulocytes (Fig. 4C, bottom panel).

Taken together, these functional assays demonstrate that $lmo2^+gata1^+CD41^+$ cells in the PBI represent a population of cells with both erythroid and myeloid differentiation potential. Their proliferation capacity is limited both in transplantation experiments and in vitro, and their progeny remain largely within in the PBI. Furthermore, they lack lymphoid potential. We therefore term these cells erythromyeloid progenitors (EMPs).
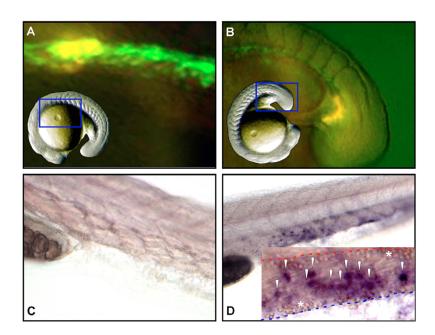
### EMPs arise independently of HSCs from caudal, $lmo2^+$ mesoderm

Collectively, our data suggest that $lmo2^+gata1^+$, or $CD41^+$ cells in the PBI before 40 hpf are committed erythromyeloid progenitors that lack self-renewal and multilineage differentiation abilities. Our

fate-mapping experiments also suggest that $CD41^+$ cells in the nascent AGM region represent the first HSCs born in the embryo. Although EMPs appear to arise before presumptive HSCs are observed in the AGM, it is possible that EMPs derive from HSCs. To determine whether EMPs are born directly in the PBI or migrate from the AGM, we performed uncaging experiments in mid-somitogenesis embryos. Approximately 10 $lmo2^+$ cells were targeted in either the medial (bounded by somites 1-10 – the region that will later contain the AGM) or most posterior portion (the region that will later become the PBI) of the stripe of mesodermal-derived tissue marked by an $lmo2:eGFP$ transgene in 13- to 15-somite-stage embryos (Fig. 5A,B). Since the number of EMPs peaks at 30 hpf (Fig. 2B), we analyzed uncaged animals at this time point. All eight animals with medial $lmo2^+$ cells targeted showed marked progeny confined to the anterior trunk region (Table 1), mainly within presumptive vasculature (not shown). None of the eight animals showed marked progeny within the PBI (Fig. 5C). Five out of eight animals with posterior $lmo2^+$ cells targeted showed marked progeny within the PBI (Table 1). These cells were large and round and localized to the vascular plexus of the PBI (Fig. 5C), consistent with our localization of $lmo2^+gata1^+$ EMPs at 30 hpf (Fig. 2A). None of these eight animals showed labeled progeny in the trunk (Table 1).



**Fig. 4. Functional studies demonstrate that $gata1^+$ $lmo2^+$ $CD41^+$ cells are committed erythromyeloid progenitors.** (**A**) Dissociated $gata1:DsRed^+$ $lmo2:eGFP^+$ cells were purified from 36 hpf embryos by flow cytometry and transplanted into wild-type embryonic recipients. Transplanted cells were observed to home back to the PBI in host animals (right panel, 200× magnification). Arrowheads denote $gata1:DsRed^+$ $lmo2:eGFP^+$ cells. (**B**) In vivo fate-mapping studies were performed by laser activation of caged rhodamine in $CD41^+$cells in the 44 hpf AGM or 40 hpf PBI. Presumptive AGM HSCs were targeted as positive controls for thymus colonization (lower panels; outlined crescent-shaped structure). Boxed yellow and blue regions in upper panel denote close-up areas shown below in left panels for the AGM and right panels for the PBI, respectively. All animals are shown in lateral view, with head oriented to the left and dorsal side up. Dotted line at the left edge of lower boxes denotes outline of the eye for orientation. White arrowheads indicate uncaged, GFP$^+$ cells. (**C**) Short-term culture of $lmo2^+$ $gata1^+$ cells atop kidney stromal cells demonstrates erythroid (E), granulocytic (G) and monocytic/macrophage (M) differentiation potentials. Cultured cells were stained for myeloperoxidase (MPX) activity after 4 days (bottom panel).

**Fig. 5. Erythromyeloid progenitors arise autonomously within the PBI.** (**A-D**) Cells expressing GFP under control of the *lmo2* promoter were lineage traced by uncaging a combination of caged rhodamine and FITC. GFP^{+} cells were targeted, either in the medial (bounded by somites 1-10; panel A) or most posterior (panel B) regions of the *lmo2* expression domain between 13- and 15-somite stages. (C,D) Analysis of targeted progeny at 30 hpf showed no medially derived cells in the PBI (C), whereas posterior-derived daughter cells were observed throughout the venous plexus of the PBI (D). Inset in (D) shows a close-up of the PBI in a second animal, with marked progeny found within the vascular plexus between the aorta (dashed red line) and caudal vein (dashed blue line). Primitive erythrocytes within each vessel are indicated with asterisks and the daughters of posterior *lmo2*^{+} cells are indicated by white arrowheads. Blue framed areas in inset images of whole animals indicate the regions shown in close-up in A and B.
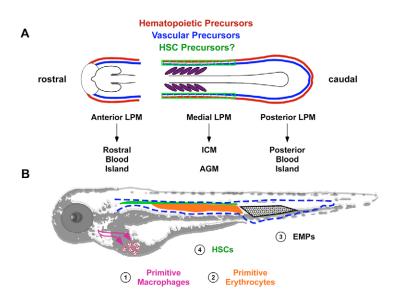
Together, these data suggest that *lmo2*[+]*gata1*[+] EMPs arise from the most posterior regions of the *lmo2*[+] (*gata1*[−]) hematopoietic or vasculogenic 'stripes' that converge to form the posterior ICM or PBI. These results are consistent with previous studies demonstrating localized expression of 'definitive' hematopoietic genes in this region such as *scl* (Liao et al., 2002) and *gata2* (Detrich et al., 1995).

## DISCUSSION

Our results demonstrate that definitive hematopoiesis initiates in the PBI through a committed progenitor that we have termed the erythromyeloid progenitor (EMP). These progenitors appear to exist transiently, between 24-48 hpf, and can be isolated prospectively by their coexpression of *lmo2* and *gata1* transgenes. Our description of a definitive progenitor in the PBI explains previous gene expression studies, which suggested that a distinct population of cells was present in the caudal most portion of the developing ICM. Based on the expression of *gata2*^{+} cells at the posterior tip of the *gata1*[+] ICM, Detrich et al. postulated these cells to be undifferentiated, presumptive hematopoietic progenitors (Detrich et al., 1995). Additional early observations showed that cells in this region also expressed *lmo2* (Thompson et al., 1998). The authors hypothesized that these cells may be the founders of a distinct second wave of hematopoiesis. Our identification of the EMP confirms these hypotheses, and characterization of their molecular markers provides the means to isolate them for functional analyses, including lineage differentiation potentials.

The presence of the EMP in the PBI by 24 hpf may help clarify the ontogeny of the definitive myeloid lineages in teleosts. Histological and ultrastructural analyses have described granulocytic precursors in the PBI, both in the zebrafish (Willett et al., 1999; Zapata et al., 2006) and carp (Rombout et al., 2005; Huttenhuis et al., 2006). We observed eosinophilic and neutrophilic granulocytes in zebrafish tail preparations by 36-48 hpf. The first granulocytes produced in the zebrafish embryo may therefore be the daughters of EMPs, and not lineally related to the primitive macrophages that arise from cephalic mesoderm. This model is consistent with the observations of Herbomel and colleagues (Herbomel et al., 1999), and with the single lineage origin of embryonic macrophages

produced in other organisms ranging from *Drosophila* to mammals (Lichanska and Hume, 2000; Evans et al., 2003). Based on the robust generation of mononuclear phagocytes by cultured EMPs, it appears that a second wave of macrophage production later occurs in the PBI through monocytic intermediates. The full differentiation potential of the EMP remains to be determined because our in vitro conditions do not appear to support all myeloerythroid lineages, including eosinophils and thrombocytes. Isolation of autologous growth factors such as Interleukin-3 and Thrombopoietin will probably be necessary to reveal the complete fate potentials of zebrafish hematopoietic stem and progenitor cells.

The first blood cells born in the mammalian embryo are erythroid cells in the extraembryonic yolk sac. Based on their resemblance to the nucleated erythrocytes of avian and amphibian species, these cells were initially termed primitive, and their enucleated embryonic counterparts definitive (McGrath and Palis, 2005). More recently, these terms have become interchangeable with yolk sac and intraembryonic hematopoiesis, respectively. The correlation of each wave with anatomical sites has led to some confusion because several reports have recently demonstrated the existence of multipotent, definitive hematopoietic precursors in the extraembryonic yolk sac that generate definitive cell types (Wong et al., 1986; Cumano, 1996; Palis et al., 1999; Bertrand et al., 2005a; Yokota et al., 2006; Yokomizo et al., 2007). Likewise, the nomenclature used for the hematopoietic waves in the zebrafish has often been inconsistent and confusing, with many publications referring to 'primitive HSCs', 'primitive granulocytes', and so forth. We propose that the same conventions applied to the murine hematopoietic waves (Keller et al., 1999; McGrath and Palis, 2005) be used to describe primitive versus definitive hematopoiesis in the zebrafish, namely that only ICM-derived erythrocytes and cephalic mesoderm-derived macrophages should be termed primitive. This nomenclature is consistent with observations in each species suggesting that the two primitive lineages appear to arise directly from mesoderm without transiting through a multipotent progenitor (Detrich et al., 1995; Herbomel et al., 1999; Keller et al., 1999; Bertrand et al., 2005a). Conversely, we propose that hematopoietic cells that derive from an oligopotent or multipotent progenitor be termed definitive.

**Fig. 6. Model of hematopoietic ontogeny in the zebrafish embryo.** (**A**) Different regions of lateral plate mesoderm (LPM) give rise to anatomically distinct regions of blood cell precursors. Drawing depicts a dorsal view of a five-somite-stage embryo. (**B**) Embryonic hematopoiesis appears to occur through four independent waves of precursor production. Each wave is numbered based on the temporal appearance of functional cells from each subset. First, primitive macrophages arise from cephalic mesoderm and migrate onto the yolk ball before spreading throughout the embryo. Second, primitive erythrocytes begin to differentiate within the intermediate cell mass (ICM) before entering circulation at approximately 24 hpf. Third, the first definitive progenitors arise as EMPs are formed within the posterior blood island (PBI). EMPs generate the first definitive myeloid cells and a new wave of erythroid cells. Finally, definitive hematopoiesis culminates with the production of multipotent HSCs between the axial vessels in the zebrafish equivalent of the AGM region.

In our current model, hematopoietic development in the zebrafish occurs in four independent waves, each through precursors that arise in different anatomical regions (Fig. 6). Two primitive waves produce macrophages from cephalic mesoderm and erythrocytes from the ICM. Likewise, two definitive waves occur, the first from EMP production in the PBI and the second from HSC generation in the AGM. It was previously proposed by Murayama and colleagues that all hematopoietic cells in the CHT derive from HSCs born in the AGM (Murayama et al., 2006). Our results do not support this hypothesis. Several lines of evidence show that hematopoietic precursors are present in the PBI before presumptive HSCs can be detected in the AGM region beginning at approximately 28 hpf. These include gene expression profiles suggestive of multilineage hematopoiesis in the PBI by 30 hpf, the appearance of definitive myelomonocytic cells within the PBI by 36 hpf, single-cell coexpression of early hematopoietic genes, such as *lmo2-gata1* or *gata1-pu.1* by 30 hpf, and *CD41:eGFP*^{+} cells appearing in the PBI before the AGM. Furthermore, our fate-mapping experiments suggest that EMPs arise directly from the *lmo2:eGFP*[+] descendents of posterior LPM that contribute to the formation of the PBI. The experiments of Murayama et al. were performed after 48 hpf. Our lineage-tracing experiments showed that *CD41:eGFP*^{+} cells in the PBI/CHT before 40 hpf lack thymus colonizing potential. After 40 hpf, we observed rare thymic immigrants from targeted *CD41:eGFP*^{+} cells in the CHT that increased in number over time. These results suggest that the first *CD41:eGFP*^{+} cells in the PBI are EMPs and that *CD41:eGFP*[+] HSCs immigrate into the nascent CHT from the AGM after 40 hpf. It appears that the EMP disappears gradually after this time, with definitive hematopoiesis in the CHT increasingly deriving from incoming HSCs. As previously suggested in the mouse, the generation of committed EMPs in the embryo before HSCs arise has probably evolved to provide a rapid burst of definitive cell types to meet the needs of the growing embryo (Keller et al., 1999; McGrath and Palis, 2005).

In conclusion, we have demonstrated that definitive hematopoiesis initiates through a committed progenitor that is generated independently of HSCs in the posterior blood island of the zebrafish embryo. These findings provide a better understanding of hematopoietic ontogeny in the zebrafish and help to clarify the beginnings of the definitive blood cell lineages in teleosts. The development of prospective isolation approaches and a variety of functional assays to both purify and distinguish EMPs and HSCs

now allows the genetic dissection of the cues that pattern each population from mesoderm. Our results also highlight the close conservation between zebrafish and mammals in the temporal development of each hematopoietic wave during development of the blood-forming system.

**References**
**Arpin, M., Friederich, E., Algrain, M., Vernel, F. and Louvard, D.** (1994). Functional differences between L- and T-plastin isoforms. *J. Cell Biol.* **127**, 1995-2008.
**Bertrand, J. Y., Jalil, A., Klaine, M., Jung, S., Cumano, A. and Godin, I.** (2005a). Three pathways to mature macrophages in the early mouse yolk sac. *Blood* **106**, 3004-3011.
**Bertrand, J. Y., Giroux, S., Golub, R., Klaine, M., Jalil, A., Boucontet, L., Godin, I. and Cumano, A.** (2005b). Characterization of purified intraembryonic hematopoietic stem cells as a tool to define their site of origin. *Proc. Natl. Acad. Sci. USA* **102**, 134-139.
**Burns, C. E., DeBlasio, T., Zhou, Y., Zhang, J., Zon, L. and Nimer, S. D.** (2002). Isolation and characterization of runxa and runxb, zebrafish members of the runt family of transcriptional regulators. *Exp. Hematol.* **30**, 1381-1389.
**Crowhurst, M. O., Layton, J. E. and Lieschke, G. J.** (2002). Developmental biology of zebrafish myeloid cells. *Int. J. Dev. Biol.* **46**, 483-492.
**Cumano, A. and Godin, I.** (2007). Ontogeny of the hematopoietic system. *Annu. Rev. Immunol.* **25**, 745-785.
**Cumano, A., Dieterlen-Lievre, F. and Godin, I.** (1996). Lymphoid potential, probed before circulation in mouse, is restricted to caudal intraembryonic splanchnopleura. *Cell* **86**, 907-916.
**Detrich, H. W., 3rd, Kieran, M. W., Chan, F. Y., Barone, L. M., Yee, K., Rundstadler, J. A., Pratt, S., Ransom, D. and Zon, L. I.** (1995). Intraembryonic hematopoietic cell migration during vertebrate development. *Proc. Natl. Acad. Sci. USA* **92**, 10713-10717.
**Dzierzak, E.** (2005). The emergence of definitive hematopoietic stem cells in the mammal. *Curr. Opin. Hematol.* **12**, 197-202.
**Evans, C. J., Hartenstein, V. and Banerjee, U.** (2003). Thicker than blood:

conserved mechanisms in Drosophila and vertebrate hematopoiesis. *Dev. Cell* **5**, 673-690.

**Ferkowicz, M. J., Starr, M., Xie, X., Li, W., Johnson, S. A., Shelley, W. C., Morrison, P. R. and Yoder, M. C.** (2003). CD41 expression defines the onset of primitive and definitive hematopoiesis in the murine embryo. *Development* **130**, 4393-4403.

**Gekas, C., Dieterlen-Lievre, F., Orkin, S. H. and Mikkola, H. K.** (2005). The placenta is a niche for hematopoietic stem cells. *Dev. Cell* **8**, 365-375.

**Godin, I., Garcia-Porrero, J. A., Dieterlen-Lievre, F. and Cumano, A.** (1999). Stem cell emergence and hemopoietic activity are incompatible in mouse intraembryonic sites. *J. Exp. Med.* **190**, 43-52.

**Hartenstein, V.** (2006). Blood cells and blood cell development in the animal kingdom. *Annu. Rev. Cell Dev. Biol.* **22**, 677-712.

**Herbomel, P., Thisse, B. and Thisse, C.** (1999). Ontogeny and behaviour of early macrophages in the zebrafish embryo. *Development* **126**, 3735-3745.

**Hsia, N. and Zon, L. I.** (2005). Transcriptional regulation of hematopoietic stem cell development in zebrafish. *Exp. Hematol.* **33**, 1007-1014.

**Hsu, K., Traver, D., Kutok, J. L., Hagen, A., Liu, T. X., Paw, B. H., Rhodes, J., Berman, J., Zon, L. I., Kanki, J. P. et al.** (2004). The pu.1 promoter drives myeloid gene expression in zebrafish. *Blood* **104**, 1291-1297.

**Hu, M., Krause, D., Greaves, M., Sharkis, S., Dexter, M., Heyworth, C. and Enver, T.** (1997). Multilineage gene expression precedes commitment in the hemopoietic system. *Genes Dev.* **11**, 774-785.

**Huang, S., Guo, Y. P., May, G. and Enver, T.** (2007). Bifurcation dynamics in lineage-commitment in bipotent progenitor cells. *Dev. Biol.* **305**, 695-713.

**Huttenhuis, H. B., Taverne-Thiele, A. J., Grou, C. P., Bergsma, J., Saeij, J. P., Nakayasu, C. and Rombout, J. H.** (2006). Ontogeny of the common carp (Cyprinus carpio L.) innate immune system. *Dev. Comp. Immunol.* **30**, 557-574.

**Jin, H., Xu, J. and Wen, Z.** (2007). Migratory path of definitive hematopoietic stem/progenitor cells during zebrafish development. *Blood* **109**, 5208-5214.

**Kalev-Zylinska, M. L., Horsfield, J. A., Flores, M. V., Postlethwait, J. H., Vitas, M. R., Baas, A. M., Crosier, P. S. and Crosier, K. E.** (2002). Runx1 is required for zebrafish blood and vessel development and expression of a human RUNX1-CBF2T1 transgene advances a model for studies of leukemogenesis. *Development* **129**, 2015-2030.

**Keller, G., Lacaud, G. and Robertson, S.** (1999). Development of the hematopoietic system in the mouse. *Exp. Hematol.* **27**, 777-787.

**Kinna, G., Kolle, G., Carter, A., Key, B., Lieschke, G. J., Perkins, A. and Little, M. H.** (2006). Knockdown of zebrafish crim1 results in a bent tail phenotype with defects in somite and vascular development. *Mech. Dev.* **123**, 277-287.

**Kosman, D., Mizutani, C. M., Lemons, D., Cox, W. G., McGinnis, W. and Bier, E.** (2004). Multiplex detection of RNA expression in Drosophila embryos. *Science* **305**, 846.

**Liao, E. C., Paw, B. H., Oates, A. C., Pratt, S. J., Postlethwait, J. H. and Zon, L. I.** (1998). SCL/Tal-1 transcription factor acts downstream of cloche to specify hematopoietic and vascular progenitors in zebrafish. *Genes Dev.* **12**, 621-626.

**Liao, E. C., Trede, N. S., Ransom, D., Zapata, A., Kieran, M. and Zon, L. I.** (2002). Non-cell autonomous requirement for the bloodless gene in primitive hematopoiesis of zebrafish. *Development* **129**, 649-659.

**Lichanska, A. M. and Hume, D. A.** (2000). Origins and functions of phagocytes in the embryo. *Exp. Hematol.* **28**, 601-611.

**Lin, H. F., Traver, D., Zhu, H., Dooley, K., Paw, B. H., Zon, L. I. and Handin, R. I.** (2005). Analysis of thrombocyte development in CD41-GFP transgenic zebrafish. *Blood* **106**, 3803-3810.

**McGrath, K. E. and Palis, J.** (2005). Hematopoiesis in the yolk sac: more than meets the eye. *Exp. Hematol.* **33**, 1021-1028.

**Meijer, A. H., van der Sar, A. M., Cunha, C., Lamers, G. E., Laplante, M. A., Kikuta, H., Bitter, W., Becker, T. S. and Spaink, H. P.** (2007). Identification and real-time imaging of a myc-expressing neutrophil population involved in inflammation and mycobacterial granuloma formation in zebrafish. *Dev. Comp. Immunol.* doi.10.1016/j.dci.2007.04.003.

**Mikkola, H. K., Fujiwara, Y., Schlaeger, T. M., Traver, D. and Orkin, S. H.** (2003). Expression of CD41 marks the initiation of definitive hematopoiesis in the mouse embryo. *Blood* **101**, 508-516.

**Mitjavila-Garcia, M. T., Cailleret, M., Godin, I., Nogueira, M. M., Cohen-Solal, K., Schiavon, V., Lecluse, Y., Le Pesteur, F., Lagrue, A. H. and Vainchenker, W.** (2002). Expression of CD41 on hematopoietic progenitors derived from embryonic hematopoietic cells. *Development* **129**, 2003-2013.

**Miyamoto, T., Iwasaki, H., Reizis, B., Ye, M., Graf, T., Weissman, I. L. and**

**Akashi, K.** (2002). Myeloid or lymphoid promiscuity as a critical step in hematopoietic lineage commitment. *Dev. Cell* **3**, 137-147.

**Murayama, E., Kissa, K., Zapata, A., Mordelet, E., Briolat, V., Lin, H. F., Handin, R. I. and Herbomel, P.** (2006). Tracing hematopoietic precursor migration to successive hematopoietic organs during zebrafish development. *Immunity* **25**, 963-975.

**Nerlov, C., Querfurth, E., Kulessa, H. and Graf, T.** (2000). GATA-1 interacts with the myeloid PU.1 transcription factor and represses PU.1-dependent transcription. *Blood* **95**, 2543-2551.

**Ottersbach, K. and Dzierzak, E.** (2005). The murine placenta contains hematopoietic stem cells within the vascular labyrinth region. *Dev. Cell* **8**, 377-387.

**Palis, J. and Yoder, M. C.** (2001). Yolk-sac hematopoiesis: the first blood cells of mouse and man. *Exp. Hematol.* **29**, 927-936.

**Palis, J., Robertson, S., Kennedy, M., Wall, C. and Keller, G.** (1999). Development of erythroid and myeloid progenitors in the yolk sac and embryo proper of the mouse. *Development* **126**, 5073-5084.

**Renshaw, S. A., Loynes, C. A., Trushell, D. M., Elworthy, S., Ingham, P. W. and Whyte, M. K.** (2006). A transgenic zebrafish model of neutrophilic inflammation. *Blood* **108**, 3976-3978.

**Rhodes, J., Hagen, A., Hsu, K., Deng, M., Liu, T. X., Look, A. T. and Kanki, J. P.** (2005). Interplay of pu.1 and gata1 determines myelo-erythroid progenitor cell fate in zebrafish. *Dev. Cell* **8**, 97-108.

**Rombout, J. H., Huttenhuis, H. B., Picchietti, S. and Scapigliati, G.** (2005). Phylogeny and ontogeny of fish leucocytes. *Fish Shellfish Immunol.* **19**, 441-455.

**Tenen, D. G., Hromas, R., Licht, J. D. and Zhang, D. E.** (1997). Transcription factors, normal myeloid development, and leukemia. *Blood* **90**, 489-519.

**Thisse, C., Thisse, B., Schilling, T. F. and Postlethwait, J. H.** (1993). Structure of the zebrafish snail1 gene and its expression in wild-type, spadetail and no tail mutant embryos. *Development* **119**, 1203-1215.

**Thompson, M. A., Ransom, D. G., Pratt, S. J., MacLennan, H., Kieran, M. W., Detrich, H. W., 3rd, Vail, B., Huber, T. L., Paw, B., Brownlie, A. J. et al.** (1998). The cloche and spadetail genes differentially affect hematopoiesis and vasculogenesis. *Dev. Biol.* **197**, 248-269.

**Traver, D., Paw, B. H., Poss, K. D., Penberthy, W. T., Lin, S. and Zon, L. I.** (2003). Transplantation and in vivo imaging of multilineage engraftment in zebrafish bloodless mutants. *Nat. Immunol.* **4**, 1238-1246.

**Westerfield, M.** (1994). *The Zebrafish Book: A Guide for the Laboratory use of Zebrafish (Brachydanio rerio).* Eugene, OR: University of Oregon Press.

**Willett, C. E., Cortes, A., Zuasti, A. and Zapata, A. G.** (1999). Early hematopoiesis and developing lymphoid organs in the zebrafish. *Dev. Dyn.* **214**, 323-336.

**Wong, P. M., Chung, S. W., Chui, D. H. and Eaves, C. J.** (1986). Properties of the earliest clonogenic hemopoietic precursors to appear in the developing murine yolk sac. *Proc. Natl. Acad. Sci. USA* **83**, 3851-3854.

**Yoder, M., Hiatt, K., Mukherjee, P.** (1997a). In vivo repopulating hematopoietic stem cells are present in the murine yolk sac at day 9.0 postcoitus. *Proc. Natl. Acad. Sci. USA* **94**, 6776-6780.

**Yoder, M. C., Hiatt, K., Dutt, P., Mukherjee, P., Bodine, D. M. and Orlic, D.** (1997b). Characterization of definitive lymphohematopoietic stem cells in the day 9 murine yolk sac. *Immunity* **7**, 335-344.

**Yokomizo, T., Takahashi, S., Mochizuki, N., Kuroha, T., Ema, M., Wakamatsu, A., Shimizu, R., Ohneda, O., Osato, M., Okada, H. et al.** (2007). Characterization of GATA-1(+) hemangioblastic cells in the mouse embryo. *EMBO J.* **26**, 184-196.

**Yokota, T., Huang, J., Tavian, M., Nagai, Y., Hirose, J., Zuniga-Pflucker, J. C., Peault, B. and Kincade, P. W.** (2006). Tracing the first waves of lymphopoiesis in mice. *Development* **133**, 2041-2051.

**Zapata, A., Diez, B., Cejalvo, T., Gutierrez-de Frias, C. and Cortes, A.** (2006). Ontogeny of the immune system of fish. *Fish Shellfish Immunol.* **20**, 126-136.

**Zeigler, B. M., Sugiyama, D., Chen, M., Guo, Y., Downs, K. M. and Speck, N. A.** (2006). The allantois and chorion, when isolated before circulation or chorio-allantoic fusion, have hematopoietic potential. *Development* **133**, 4183-4192.

**Zhang, P., Zhang, X., Iwama, A., Yu, C., Smith, K. A., Mueller, B. U., Narravula, S., Torbett, B. E., Orkin, S. H. and Tenen, D. G.** (2000). PU.1 inhibits GATA-1 function and erythroid differentiation by blocking GATA-1 DNA binding. *Blood* **96**, 2641-2648.

**Zhu, H., Traver, D., Davidson, A. J., Dibiase, A., Thisse, C., Thisse, B., Nimer, S. and Zon, L. I.** (2005). Regulation of the lmo2 promoter during hematopoietic and vascular development in zebrafish. *Dev. Biol.* **281**, 256-269.